Dark Matter and CP-violation in the Three-Higgs Doublet Model

2017 J. Phys.: Conf. Ser. 873 012030

(http://iopscience.iop.org/1742-6596/873/1/012030)

IOP Conf. Series: Journal of Physics: Conf. Series **873** (2017) 012030 doi:10.1088/1742-6596/873/1/012030

Dark Matter and CP-violation in the Three-Higgs Doublet Model

Dorota Sokołowska

University of Warsaw, Faculty of Physics, Pasteura 5, 02-093 Warsaw, Poland.

E-mail: dsok@fuw.edu.pl

Abstract. In many scalar Dark Matter models an imposed discrete symmetry will result in CP conservation. We present results for the 3HDM, the Standard Model with two additional inert doublets, where it is possible to have CP-violating effects and a stable Dark Matter candidate. We discuss the new regions of DM relic density opened up by CP-violation and constrain the parameter space of the CP-violating model using recent results from the LHC and DM direct and indirect detection experiments.

1. Introduction

In 2012 a scalar boson with a mass of ≈ 125 GeV was discovered by both ATLAS and CMS experiments at the CERN Large Hadron Collider (LHC) reported [1, 2]. Although the properties of the observed boson are in accordance with those of the Higgs boson of the Standard Model (SM), it may just be one member of an extended scalar sector. So far no signs of detection of physics Beyond SM (BSM) have been reported, but it is well understood that the SM of particle physics is not complete. A good motivation for BSM is the lack of a Dark Matter (DM) candidate in the SM. Although the nature of DM is not yet known, according to the Standard Cosmological Λ-CDM Model it should be a particle which is stable on cosmological time scales, cold, non-baryonic, neutral and weakly interacting. Various candidates for such a state with these characteristics exist in the literature, the most well-studied being Weakly Interacting Massive Particles (WIMPs) [3, 4, 5]. Any such WIMP candidate must be cosmologically stable, usually due to the conservation of a discrete symmetry, and must freeze-out to result in the observed relic density of $\Omega_{\rm DM}h^2 = 0.1199 \pm 0.0027$ [6].

It is clear that the SM scalar sector cannot provide a WIMP candidate. However, it was suggested some time ago that the scalar sector could be extended by the addition of an extra doublet, which may not develop a Vacuum Expectation Value (VEV) while leaving a discrete Z_2 symmetry unbroken [7]. This possibility, which is known as the Inert Doublet Model (IDM), has been studied extensively for the last few years (see, e.g., [8, 9, 10]). Since the IDM involves *1 inert* doublet plus *1 active* Higgs doublet, we shall also refer to it as the I(1+1)HDM.

The I(1+1)HDM remains a viable model for a scalar DM candidate, being in agreement with current experimental constraints, although the allowed parameter space is reduced [11, 12, 13].

In recent papers [14, 15] we studied DM in a model with *2* inert plus *1* active Higgs doublet, which we referred to as the I(2+1)HDM. We showed that the extended scalar sector can provide a viable DM candidate in a region of parameter space which would be excluded in the I(1+1)HDM.

In this work we present results for chosen benchmarks for the CP-violating I(2+1)HDM [16]. We found that introduction of complex parameters in the scalar potential changes the annihilation scenarios of the DM candidate, opening new regions of parameter space in agreement with all experimental constraints.

2. The scalar sector of 3HDM

Here we discuss a particular version of a 3HDM with *2* inert and *1* active doublet, which we refer to as the I(2+1)HDM. Let us define a Z_2 symmetry under which the three scalar doublets $\phi_{1,2,3}$ transform, respectively, as $g_{Z_2} = \mathrm{diag}\,(-1,-1,1)$. A Z_2-symmetric 3HDM potential[1] is of the following form [17] :

$$\begin{aligned} V_{3HDM} \;=\; & -\mu_1^2(\phi_1^\dagger\phi_1) - \mu_2^2(\phi_2^\dagger\phi_2) - \mu_3^2(\phi_3^\dagger\phi_3) + \lambda_{11}(\phi_1^\dagger\phi_1)^2 + \lambda_{22}(\phi_2^\dagger\phi_2)^2 + \lambda_{33}(\phi_3^\dagger\phi_3)^2 \\ & +\lambda_{12}(\phi_1^\dagger\phi_1)(\phi_2^\dagger\phi_2) + \lambda_{23}(\phi_2^\dagger\phi_2)(\phi_3^\dagger\phi_3) + \lambda_{31}(\phi_3^\dagger\phi_3)(\phi_1^\dagger\phi_1) \\ & +\lambda'_{12}(\phi_1^\dagger\phi_2)(\phi_2^\dagger\phi_1) + \lambda'_{23}(\phi_2^\dagger\phi_3)(\phi_3^\dagger\phi_2) + \lambda'_{31}(\phi_3^\dagger\phi_1)(\phi_1^\dagger\phi_3), \\ & -\mu_{12}^2(\phi_1^\dagger\phi_2) + \lambda_1(\phi_1^\dagger\phi_2)^2 + \lambda_2(\phi_2^\dagger\phi_3)^2 + \lambda_3(\phi_3^\dagger\phi_1)^2 + h.c. \end{aligned}$$

where CP violation (CPV) is introduced explicitly through complex parameters of the potential: $\mu_{12}^2, \lambda_{1,2,3}$. Here, we study a simplified version of the I(2+1)HDM by imposing the following equalities $\mu_1^2 = \mu_2^2, \lambda_3 = \lambda_2, \lambda_{31} = \lambda_{23}, \lambda'_{31} = \lambda'_{23}$ which we call the "dark democracy" limit. By imposing it, there are only two parameters that remain complex[2]: $\mu_{12}^2 = |\mu_{12}^2|e^{i\theta_{12}}$ and $\lambda_2 = |\lambda_2|e^{i\theta_2}$; θ_{12} and θ_2 as the respective CPV phases. Note that the *inert* sector is protected by a conserved Z_2 symmetry from coupling to the SM particles, therefore, the amount of CPV introduced here is not constrained by SM data.

The doublets are defined as

$$\phi_1 = \begin{pmatrix} H_1^+ \\ \frac{H_1^0+iA_1^0}{\sqrt{2}} \end{pmatrix}, \quad \phi_2 = \begin{pmatrix} H_2^+ \\ \frac{H_2^0+iA_2^0}{\sqrt{2}} \end{pmatrix}, \quad \phi_3 = \begin{pmatrix} G^+ \\ \frac{v+h+iG^0}{\sqrt{2}} \end{pmatrix}, \tag{1}$$

where ϕ_1 and ϕ_2 are the two doublets that are odd under the Z_2 (hence are inert) and ϕ_3 is the active doublet, which is even under the Z_2 and plays the role of the SM-Higgs doublet. The symmetry of the potential is therefore respected by the vacuum alignment.

To make the entire Lagrangian Z_2-symmetric, an even Z_2 parity is assigned to all SM particles, identical to the Z_2 parity of the only doublet that couples to them, i.e., the active doublet ϕ_3 [18] (the Yukawa Lagrangian of the model is identical to the SM Yukawa Lagrangian). With this parity assignment Flavour Changing Neutral Currents are avoided as the extra doublets are forbidden to couple to fermions by Z_2 conservation. Furthermore, the conservation of Z_2-symmetry leads to the lightest particle from doublets $\phi_{1,2}$ to be stable. Among the Z_2-odd particles there are four neutral states, S_i, and two charged states, $S_i^\pm$.

The neutral physical states are composed of all neutral base states from (1), so have a mixed CP-charge. We take S_1 to be the lightest neutral field from the inert doublets:

$$\begin{aligned} S_1 &= \frac{\alpha H_1^0 + \alpha H_2^0 - A_1^0 + A_2^0}{\sqrt{2\alpha^2+2}}, \quad S_2 = \frac{-H_1^0 - H_2^0 - \alpha A_1^0 + \alpha A_2^0}{\sqrt{2\alpha^2+2}}, \\ S_3 &= \frac{\beta H_1^0 - \beta H_2^0 + A_1^0 + A_2^0}{\sqrt{2\beta^2+2}}, \quad S_4 = \frac{-H_1^0 + H_2^0 + \beta A_1^0 + \beta A_2^0}{\sqrt{2\beta^2+2}}, \end{aligned} \tag{2}$$

[1] Adding extra Z_2-respecting terms e.g. $(\phi_3^\dagger\phi_1)(\phi_2^\dagger\phi_3), (\phi_1^\dagger\phi_2)(\phi_3^\dagger\phi_3), (\phi_1^\dagger\phi_2)(\phi_1^\dagger\phi_1)$ and/or $(\phi_1^\dagger\phi_2)(\phi_2^\dagger\phi_2)$ does not change the phenomenology of the model. The coefficients of these terms, therefore, are set to zero for simplicity.

[2] The remaining parameter, λ_1 governs the self-coupling of inert particles and does not influence DM or LHC phenomenology studied here.

where α and β are the rotation angles [16].

Note that the scalar h contained in the doublet ϕ_3 in our model, has exactly the couplings of the SM-Higgs boson. The CP-violation is only introduced in the *inert* sector which is forbidden from mixing with the *active* sector by the Z_2 symmetry. Therefore, the amount of CP-violation is not limited by EDMs and SM-Higgs couplings.

It is useful to write the parameters of the model in terms of the physical observables:

$$|\mu_{12}^2| = \frac{1}{2}(m_{S_2^\pm}^2 - m_{S_1^\pm}^2), \lambda_{23} = \frac{2\mu_2^2}{v^2} + \frac{m_{S_2^\pm}^2 + m_{S_1^\pm}^2}{v^2}, \lambda'_{23} = \frac{1}{v^2}(m_{S_2}^2 + m_{S_1}^2 - m_{S_2^\pm}^2 - m_{S_1^\pm}^2),$$
$$\mu_2^2 = \frac{v^2}{2} g_{S_1 S_1 h} - \frac{v^2|\lambda_2|}{2(1+\alpha^2)}\Big(4\alpha \sin\theta_2 + 2(\alpha^2-1)\cos\theta_2\Big) - \frac{m_{S_2}^2 + m_{S_1}^2}{2},$$
$$|\lambda_2| = \frac{1}{v^2}\left[|\mu_{12}^2|\cos(\theta_2+\theta_{12}) + \sqrt{|\mu_{12}^2|^2\cos^2(\theta_2+\theta_{12}) + \left(\frac{m_{S_2}^2 - m_{S_1}^2}{2}\right)^2 - |\mu_{12}^2|^2}\right].$$

We take the masses of $S_{1,2}, S_{1,2}^\pm$, the two angles θ_2 and θ_{12} and the Higgs-DM coupling, $g_{S_1 S_1 h}$ (with the Lagrangian term equal to $\frac{v}{2} g_{S_1 S_1 h} h S_1^2$) as the input parameters of the model.

2.1. Constraints on parameters

We take into account various theoretical and experimental constraints that include: the boundedness of the potential, positive-definiteness of the Hessian and S, T, U parameters put on the model, bounds from relic density observations, Gamma-ray searches, DM direct and indirect detection, the contribution of the new scalars to the W and Z gauge boson widths, null searches for charged scalars at LEP and LHC, invisible Higgs decays, Higgs total decay width and the $h \to \gamma\gamma$ signal strength [16].

3. Relevant DM (co)annihilation scenarios

The relic density of the scalar DM candidate, S_1, after freeze-out is given by the solution of the Boltzmann equation:

$$\frac{dn_{S_1}}{dt} = -3Hn_{S_1} - \langle\sigma_{eff} v\rangle(n_{S_1}^2 - n_{S_1}^{eq\,2}), \tag{3}$$

where the thermally averaged effective (co)annihilation cross section contains all relevant annihilation processes of any $S_i S_j$ pair into SM particles:

$$\langle\sigma_{eff} v\rangle = \sum_{ij}\langle\sigma_{ij} v_{ij}\rangle \frac{n_i^{eq}}{n_{S_1}^{eq}}\frac{n_j^{eq}}{n_{S_1}^{eq}}, \quad \frac{n_i^{eq}}{n_{S_1}^{eq}} \sim \exp(-\frac{m_i - m_{S_1}}{T}). \tag{4}$$

Therefore, only processes for which the mass splitting between S_i and the lightest Z_2-odd particle S_1 are comparable to the thermal bath temperature T provide a sizeable contribution to this sum.

The I(2+1)HDM studied here has many features of a Higgs-portal DM model. In a large region of parameter space the crucial DM annihilation channel is $S_1 S_1 \to h \to f\bar{f}$, with the cross-section depending on both the mass of DM and the Higgs-DM coupling. In general, if $m_{\rm DM} < m_h/2$, then a relatively large coupling is needed to produce correct relic density. Processes that produce gauge boson, e.g. $S_1 S_1 \to h \to VV, S_1 S_1 \to VV$, where V is any of the SM gauge bosons, also contribute to the total annihilation cross section. These contributions are suppressed when m_{S_1} is smaller than m_W, however it is known that diagrams with off-shell gauge bosons may be very important.

Coannihilation effects play an important role in scenarios with multiple particles that are close in mass. Therefore, processes such as $S_1S_i \to h \to f\bar{f}, S_1S_i \to Z^* \to f\bar{f}, S_1S_j^{\pm} \to W^{\pm *} \to ff'$ with $i = 2, 3, 4$ and $j = 1, 2$ are included in calculating the effective annihilation cross section. If all inert particles are very close in mass then all channels $S_iS_j \to h \to f\bar{f}, S_iS_j \to VV$ contribute to the final DM relic density.

Below we present the numerical results for the chosen benchmark scenarios for low and medium DM mass. It is convenient to introduce the mass splittings between the DM candidate and other inert scalars as: $\delta_{12} = m_{S_2} - m_{S_1}$, $\delta_{1c} = m_{S_1^{\pm}} - m_{S_1}$, $\delta_c = m_{S_1^{\pm}} - m_{S_2^{\pm}}$, with the CP-violating phases complementing the needed parameter set of $m_{S_{1,2}}, m_{S_{1,2}^{\pm}}$ θ_2 and θ_{12}. We then define three base benchmarks in low and medium mass region as:

$$A1: \ \delta_{12} = 125\,\text{GeV}, \delta_{1c} = 50\,\text{GeV}, \delta_c = 50\,\text{GeV}, \theta_2 = \theta_{12} = 1.5 \tag{5}$$

$$B1: \ \delta_{12} = 125\,\text{GeV}, \delta_{1c} = 50\,\text{GeV}, \delta_c = 50\,\text{GeV}, \theta_2 = \theta_{12} = 0.82 \tag{6}$$

$$C1: \ \delta_{12} = 12\,\text{GeV}, \delta_{1c} = 100\,\text{GeV}, \delta_c = 1\,\text{GeV}, \theta_2 = \theta_{12} = 1.57 \tag{7}$$

In the case of **Scenario A**, where there are large mass splittings between the DM candidate and all other inert particles ($m_{S_1} \ll m_{S_2}, m_{S_3}, m_{S_4}, m_{S_1^{\pm}}, m_{S_2^{\pm}}$), no co-annihilation channels are present. In **Scenario B**, where $m_{S_1} \sim m_{S_3} \ll m_{S_2}, m_{S_4}, m_{S_1^{\pm}}, m_{S_2^{\pm}}$, the DM candidate can coannihilate with its only particle close in mass, namely S_3. In **Scenario C**, with all neutral particles close in mass, $m_{S_1} \sim m_{S_3} \sim m_{S_2} \sim m_{S_4} \ll m_{S_1^{\pm}}, m_{S_2^{\pm}}$, the DM particle can coannihilate with all other neutral inert particles.

4. Relation between couplings and DM relic density

In the CP-conserving version of the I(2+1)HDM (within the "dark democracy" limit) [14, 15], couplings between inert scalars and gauge bosons are fixed, and given by the rotation angles $\theta_a = \theta_h = \pi/4$. They do not depend on the mass splittings or the value of m_{S_1}. In the CP-violating case the situation is different, as the couplings (normalized to $\frac{ie}{2c_w s_w}$) are given by:

$$\chi_{ZS_1S_3} = \chi_{ZS_2S_4} = \frac{\alpha + \beta}{\sqrt{\alpha^2 + 1}\sqrt{\beta^2 + 1}}, \chi_{ZS_1S_4} = \chi_{ZS_2S_3} = \frac{\alpha\beta - 1}{\sqrt{\alpha^2 + 1}\sqrt{\beta^2 + 1}}, \tag{8}$$

$$\chi^2_{ZS_1S_3} + \chi^2_{ZS_1S_4} = 1, \quad \chi^2_{ZS_2S_3} + \chi^2_{ZS_2S_4} = 1. \tag{9}$$

The strength of gauge-inert interaction depends on parameters α and β, which in turn depend on m_{S_i}. Higgs-inert scalar couplings are also modified with respect to the CP-conserving case [16]. This leads to important differences in DM phenomenology, especially in the region where coannihilation channels are important. Fig. 1 shows the change in values of Z-inert couplings for benchmarks A1, B1 and C1. The introduction of varying values of α and β leads to the following modifications with respect to the (co)annihilation scenarios in the CP-conserving I(2+1)HDM.

4.1. Low DM mass region

For benchmark A1, couplings with the Z boson are modified with respect to the CP-conserving case (Fig. 1), however, as DM does not coannihilate, it does not change the annihilation scenario of S_1. For low DM mass S_1 annihilates mostly through $S_1S_1 \to h \to b\bar{b}$, entering the resonance region with small Higgs-DM coupling for masses close to $m_h/2$. This benchmark resembles both the CP-conserving I(2+1)HDM as well as the IDM.

For benchmark B1, S_1 is close in mass with S_3, opening the coannihilation channel $S_1S_3 \to Z \to f\bar{f}$. Such a scenario in the CP-conserving limit results in too low a relic density for any value of the Higgs-DM coupling due to strong coannihilation. However, in the CP-violating case its strength is reduced. We can therefore change the contribution of this diagram to the

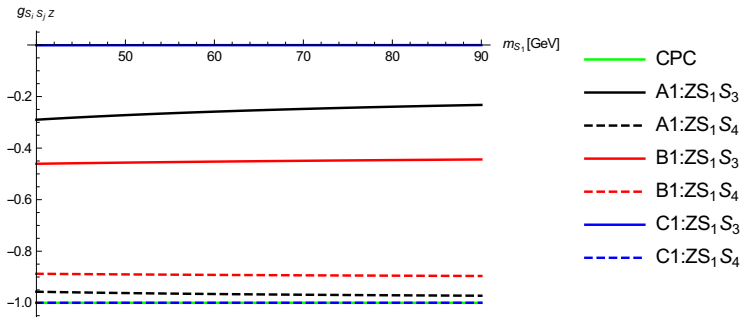

Figure 1. $\chi_{ZS_1S_3} = \chi_{ZS_2S_4}$ and $\chi_{ZS_1S_4} = \chi_{ZS_2S_3}$ for chosen benchmarks. Figure from [16].

relic density calculations not only by introducing the change for the mass splitting, but also by modifying the value of the coupling itself.

For benchmark C1 all particles are close in mass and in principle all coannihilation diagrams could be important. The couplings $g_{S_1S_2h}, g_{S_3S_4h}$ and $g_{ZS_1S_3}$ are suppressed, and the crucial contribution comes from $S_1S_4 \to Z \to q\bar{q}$. In the CP-conserving case, this scenario is only viable in the resonance region, but in the CP-violating case the strength of the coannihilation channels depends on the input parameters and can therefore vary.

Figure 2 shows good relic density regions in the $(m_{S_1}, g_{S_1S_1h})$ plane for benchmarks A1, B1 and C1. Benchmark A1 exhibits the standard behaviour of an $SU(2)$ DM candidate. For benchmark B1 coannihilation channels are important, unlike A1. For large values of $g_{S_1S_1h}$ the dominant channel is $S_1S_1 \to h \to \bar{b}b$ and, as there are also coannihilation channels, $\Omega_{DM}h^2$ is usually too small. For smaller couplings the dominant channel is $S_1S_3 \to Z \to q\bar{q}$, especially strong for low masses. As the mass grows, the coannihilation channel gets weaker, allowing us to obtain the proper relic density. For masses closer to $m_h/2$ the Higgs resonance annihilation dominates. In case of benchmark C1 for small values of $g_{S_1S_1h}$ the dominant channel is $S_1S_4 \to Z \to f\bar{f}$ (light quarks), with a small contribution from $S_2S_3 \to Z \to f\bar{f}$. For larger couplings the process $S_1S_1 \to h \to b\bar{b}$ strongly increases the annihilation cross section. This, combined with the fact that coannihilation channels are generally strong, leaves the region $m_{S_1} > 49$ GeV.

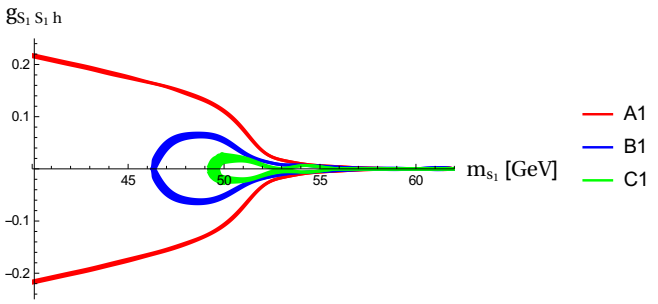

Figure 2. Relic density for low DM mass region in Scenarios A1, B1 and C1. Figure from [16].

4.2. Medium DM mass region

Here, for $m_h/2 < m_{S_1} < m_{W^\pm,Z}$, the crucial channel for all benchmarks is the annihilation of $S_1S_1 \to W^+W^-$ and this vertex does not depend on parameters α and β, but only the

DM mass. This is why all studied benchmarks, as well as the CP-conserving scenarios, follow the similar behaviour, presented in Fig. 3. For larger values of DM mass this annihilation is stronger, and cancellation with $S_1S_1 \to h \to W^+W^-$ is needed to ensure the proper value of relic density. This mechanism is responsible for moving towards negative values of Higgs-DM coupling. In benchmarks B1 and C1 other channels, like $S_1S_4 \to q\bar{q}$ or $S_3S_3 \to W^+W^-$ give small contributions, leading to small deviations from the behaviour of benchmark A1.

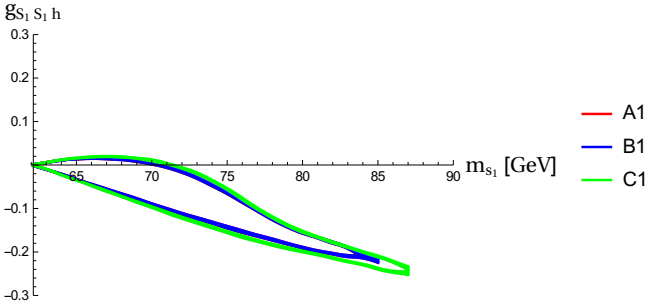

Figure 3. Relic density for medium DM mass region in Scenarios A1, B1 and C1. Note that the medium mass region behaviour of the three scenarios is very similar to each other. Figure from [16].

4.3. Other solutions in low and medium mass region

In the discussion above we have presented results for three sets of parameters in scenarios A1, B1, and C1. By changing the input parameter set we can reach different regions of parameters space. The performed scan shows that by varying the mass splitting and phases θ_2 and θ_{12} we can actually fill the empty regions in plots 2 and 3 within the range given by the CP-conserving scenario with large mass splittings (the standard SU(2) DM candidate, with no coannihilation channels). There is more freedom in the low mass region, as the strength of coannihilation channels depends strongly on α and β. In the medium mass region main annihilation of S_1 into WW pair (both direct and Higgs-mediated) is benchmark independent and the coannihilation processes have smaller impact.

In Fig. 4 results obtained for various additional sets of parameters are presented. We can fill the plot by different B scenarios, where the coannihilation channel $S_1S_3 \to Z \to q\bar{q}$ (with varying $\chi_{ZS_1S_3}$) is crucial. There are also multiple solutions of type C, where all neutral particles have a relatively low mass.

4.4. DM detection experiments

DM direct detection experiments aim to measure the scattering of DM particle off nuclei. This interaction is mediated by the Higgs particle, and therefore results of these experiments constrain the DM mass, as well as its coupling to h. In the low and medium mass region the strongest constraints come from the LUX experiment [19], and they set strong limits on the parameter space of the 3HDM. Results are presented in Fig. 5, where the solid line corresponds to the current LUX limit, while the dashed line shows the projected sensitivity of XENON1T [20]. From the plot we can see that for chosen benchmark points A1, B1 and C1 the only surviving region of this part of parameter space is $50\,\text{GeV} \lesssim m_{S_1} \lesssim 76\,\text{GeV}$, where the Higgs-DM coupling can be small. From Fig. 5 one can see that a large part of parameter space is within the reach of future experiments, however there are still points, which correspond to $g_{S_1S_1h} \to 0$ that will escape detection.

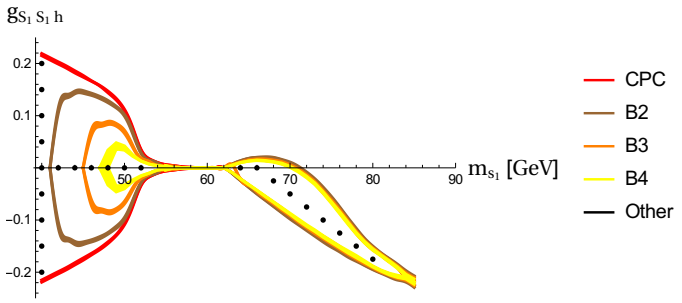

Figure 4. The relic density plots for different B and C scenarios where by changing the angles θ_2 and θ_{12} the whole region not accesible by the CP-conserving limit could be realised in the CP-violating case. Figure from [16].

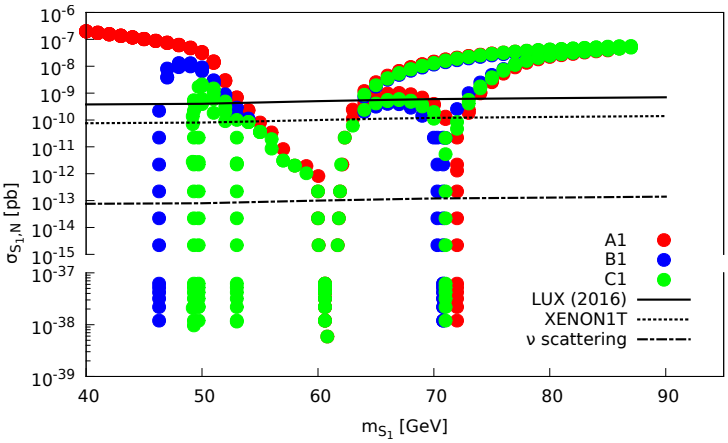

Figure 5. Direct detection limits for low and medium mass regions. Figure from [16].

Recent indirect detection results from Fermi-LAT strongly constrain the DM candidate annihilating into $b\bar{b}$ pair [21], and therefore are crucial for the low DM mass region. The CP-conserving scalar Higgs-portal type of DM with proper relic density and $m_{S_1} \lesssim 53$ GeV is ruled out. The same limit applies to case A1, as the dominant annihilation channel is into $b\bar{b}$ pair (Figure 6). For cases B1 and C1 annihilation channels are different and a good relic density is obtained for smaller values of Higgs-DM coupling. This weakens the annihilation into $b\bar{b}$, leading to most of the parameter space to lie within the allowed region, see Fig. 6.

In both direct and indirect detection plots one can see two branches in the medium mass region correspond to two asymmetrical regions from Fig. 3. They do overlap in the low mass region, where good relic density regions from Fig. 2 are symmetrical. Direct and indirect detection experiments provide a complementary way to constrain the parameter space of the model. It is especially important for masses just above $m_h/2$, where the Higgs-DM coupling is small. This region escapes the possibility of direct detection, however, due to an enhancement from the Breit-Wigner resonance effect it is possible to exclude this region from the results of indirect detection experiments.

4.5. LHC limits

The presence of additional light scalars can modify decays of the Higgs particle. Channel $h \to S_1 S_1$ contributes to the Higgs invisible decay ratio (BR($h \to$ inv.)), as S_1 is stable and will

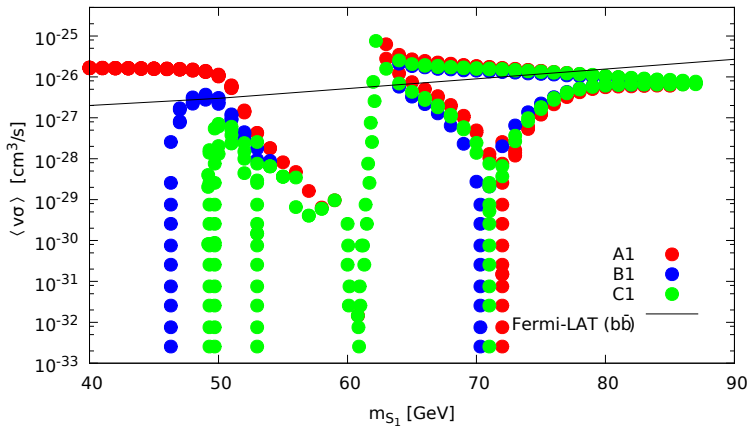

Figure 6. Indirect detection limits for low and medium mass region. Figure from [16].

escape the detector. All other inert particles can contribute to the total decay width of h (μ_{tot}). Results for benchmarks A1, B1, C1, as well as the experimental limits [22, 23, 24], are presented in Fig. 7, 8, 9. In case A1 there is only one particle that contributes to the Higgs decay (the DM candidate S_1). For small values of $g_{S_1S_1h}$ the contribution to the total decay width of the Higgs particle, and its invisible branching ratio, is small enough. There is also a small region fulfilling this constraint for case C1, but not for case B1. This is related to especially large values of $g_{S_iS_ih}$ couplings in case B, that significantly change decay channels of the Higgs particle with respect to the SM case.

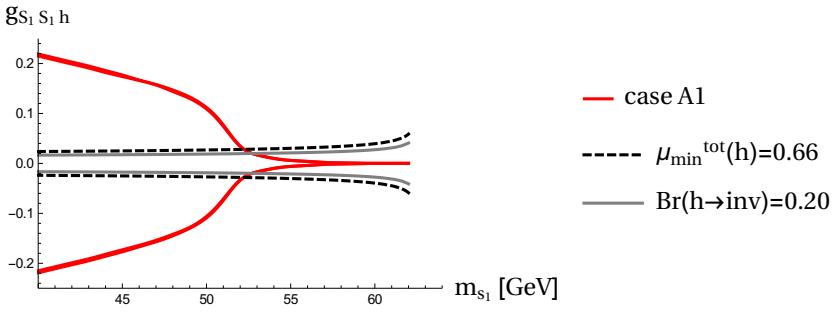

Figure 7. Relic density constraints vs. Higgs invisible branching ratio and Higgs total signal strength bounds for scenario A1. Figure from [16].

We want to stress that the LHC limits can provide stronger constraints for some benchmark points in the low mass region than the dedicated DM detection experiments. It is especially important considering the astrophysical uncertainties that may influence interpretation of results provided by DM detection experiments.

5. Conclusion

In this paper we have studied an extension of the Standard Model (SM) in which two copies of the SM-Higgs doublet which do not acquire a Vacuum Expectation Value (VEV), and hence are *inert*, are added to the scalar sector. In other words, this is a 3HDM with two inert and one active scalar doublet, denoted as the I(2+1)HDM. We have allowed for CP-violation in the

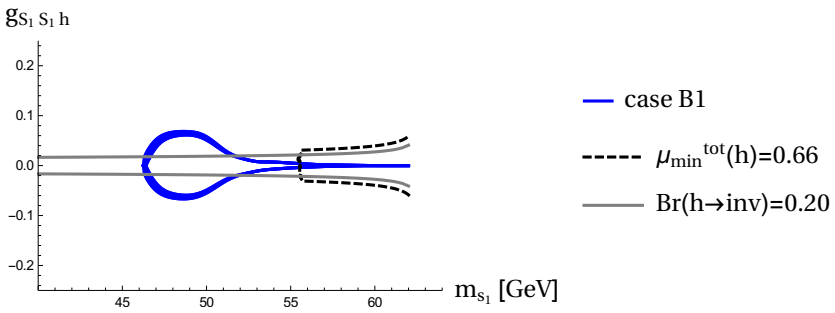

Figure 8. Relic density constraints vs. Higgs invisible branching ratio and Higgs total signal strength bounds for scenario B1. Figure from [16].

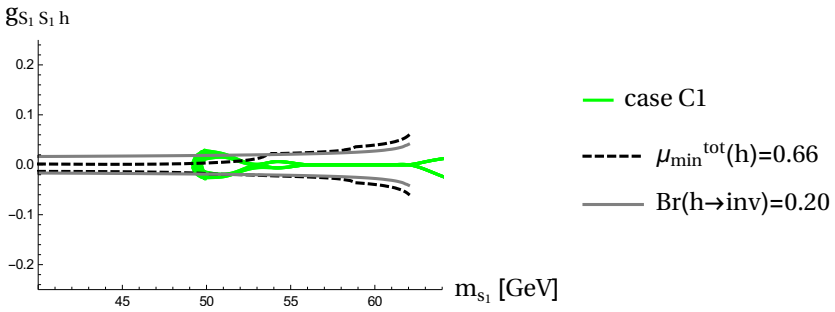

Figure 9. Relic density constraints vs. Higgs invisible branching ratio and Higgs total signal strength bounds for scenario C1. Figure from [16].

inert sector, where the lightest *inert* state is protected from decaying to SM particles through the conservation of a Z_2 symmetry. The lightest neutral particle from the *inert* sector, which has a mixed CP-charge due to CP-violation, is hence a DM candidate in the model.

The extended scalar sector, and the inclusion of complex parameters in the scalar potential, accommodates both the DM candidate and an unbounded amount of possible CPV. We find that with the introduction of CP violation, the strength of the gauge-inert couplings which were fixed in the CP conserving limit, become unconstrained, allowing us for more freedom and giving the access to a previously excluded part of parameter space. In particular, it is possible to have a light DM candidate, with very small DM-Higgs coupling, that is in agreement with all experimental data, unlike in the previously studied the I(1+1)HDM or CP-conserving I(2+1)HDM.

Acknowledgement
DS is partially supported by the HARMONIA project under contract UMO-2015/18/M/ST2/00518 (2016-2019).

References
[1] Aad G *et al.* (ATLAS) 2012 *Phys. Lett.* **B716** 1–29 (*Preprint* 1207.7214)
[2] Chatrchyan S *et al.* (CMS) 2012 *Phys. Lett.* **B716** 30–61 (*Preprint* 1207.7235)
[3] Jungman G, Kamionkowski M and Griest K 1996 *Phys. Rept.* **267** 195–373 (*Preprint* hep-ph/9506380)
[4] Bertone G, Hooper D and Silk J 2005 *Phys. Rept.* **405** 279–390 (*Preprint* hep-ph/0404175)
[5] Bergstrm L 2000 *Rept. Prog. Phys.* **63** 793 (*Preprint* hep-ph/0002126)
[6] Ade P A R *et al.* (Planck) 2016 *Astron. Astrophys.* **594** A13 (*Preprint* 1502.01589)
[7] Deshpande N G and Ma E 1978 *Phys.Rev.* **D18** 2574

[8] Ma E 2006 *Phys. Rev.* **D73** 077301 (*Preprint* hep-ph/0601225)
[9] Barbieri R, Hall L J and Rychkov V S 2006 *Phys. Rev.* **D74** 015007 (*Preprint* hep-ph/0603188)
[10] Lopez Honorez L, Nezri E, Oliver J F and Tytgat M H G 2007 *JCAP* **0702** 028 (*Preprint* hep-ph/0612275)
[11] Krawczyk M, Sokolowska D, Swaczyna P and Swiezewska B 2013 *JHEP* **09** 055 (*Preprint* 1305.6266)
[12] Arhrib A, Tsai Y L S, Yuan Q and Yuan T C 2014 *JCAP* **1406** 030 (*Preprint* 1310.0358)
[13] Ilnicka A, Krawczyk M and Robens T 2016 *Phys. Rev.* **D93** 055026 (*Preprint* 1508.01671)
[14] Keus V, King S F, Moretti S and Sokolowska D 2014 *JHEP* **11** 016 (*Preprint* 1407.7859)
[15] Keus V, King S F, Moretti S and Sokolowska D 2015 *JHEP* **11** 003 (*Preprint* 1507.08433)
[16] Cordero-Cid A, Hernndez-Snchez J, Keus V, King S F, Moretti S, Rojas D and Sokołowska D 2016 *JHEP* **12** 014 (*Preprint* 1608.01673)
[17] Ivanov I P, Keus V and Vdovin E 2012 *J. Phys.* **A45** 215201 (*Preprint* 1112.1660)
[18] Ivanov I P and Keus V 2012 *Phys. Rev.* **D86** 016004 (*Preprint* 1203.3426)
[19] Akerib D S *et al.* (LUX) 2017 *Phys. Rev. Lett.* **118** 021303 (*Preprint* 1608.07648)
[20] Aprile E (XENON1T) 2013 *Springer Proc. Phys.* **148** 93–96 (*Preprint* 1206.6288)
[21] Ackermann M *et al.* (Fermi-LAT) 2015 *Phys. Rev. Lett.* **115** 231301 (*Preprint* 1503.02641)
[22] Aad G *et al.* (ATLAS) 2015 *JHEP* **11** 206 (*Preprint* 1509.00672)
[23] Collaboration C (CMS) 2015
[24] Olive K A *et al.* (Particle Data Group) 2014 *Chin. Phys.* **C38** 090001